Brazilian Journal of Physics
ISSN: 0103-9733
luizno.bjp@gmail.com
Sociedade Brasileira de Física
Brasil

Teixeira Dias, Fabio; Lincoln Brum, Leite Gusmão Pinheiro; Alcione Roberto, Jurelo
Raman Spectroscopy of Ba(Fe1xMnx)2As2
Brazilian Journal of Physics, vol. 45, núm. 2, abril, 2015, pp. 238-243
Sociedade Brasileira de Física
São Paulo, Brasil

Braz J Phys (2015) 45:238–243
DOI 10.1007/s13538-015-0310-6

CONDENSED MATTER

# Raman Spectroscopy of $Ba(Fe_{1-x}Mn_x)_2As_2$

**Fabio Teixeira Dias · Lincoln Brum Leite Gusmão Pinheiro · Alcione Roberto Jurelo**

Received: 23 January 2015 / Published online: 7 March 2015


**Abstract** Raman scattering measurements on iron–pnictide Mn-doped $BaFe_2As_2$ single crystals are reported. Single crystals were grown out of a FeAs self-flux using conventional high-temperature solution growth and characterized by X-ray diffraction, atomic force microscopy, and Raman. Raman spectra were obtained at room temperature and 77 K on *ab*- and *a*(*b*)*c*-planes. Two of four phonon modes allowed by symmetry were found and identified. It was observed that the scattering intensity of $A_{1g}$ mode and the frequencies of the $A_{1g}$ and $B_{1g}$ phonons are dependent upon doping of Mn. The dependence of scattering intensity and frequency of $A_{1g}$ mode on Mn doping might indicate that the Mn ion also occupies the As site.

**Keywords** Iron-based superconductor · Single crystal · Manganese · Raman spectroscopy

## 1 Introduction

Since the discovery of superconductivity in iron–arsenides, much effort has been devoted both to exploring their physical properties and to the search for new materials. Up to now, a variety of iron-based superconductors such as 1111 (REFeAs(O,F)) [1, 2], 122 ((Ba,K)$Fe_2As_2$) [3], 11 (Fe(Se, Te)) [4], and 111 (LiFeAs) [5–7] were discovered. They are particularly suitable systems to study the interplay between the structural, magnetic, and superconducting orders. The 122 ternary iron arsenide has emerged as one of the most important systems because large flux-grown single crystals can be readily obtained.

Superconductivity occurs in the $BaFe_2As_2$ compound by hole doping [8, 9] and with critical temperature $T_C$ values up to 38 K for K-doped [3]. Also, upon cooling, a structural phase transition takes place ($T_S$=173 K) from the high-temperature tetragonal to the low-temperature orthorhombic (*Fmmm*) phase [3]. Electron-doped $Ba(Fe_{1-x}Co_x)_2As_2$ is another suitable system, and unlike the substitution of $Ba^{2+}$ for $K^+$ ions, Co has advantages as dopant since carriers are added directly into the FeAs planes [10]. In the special case of Mn, although it is adjacent to Fe in the periodic table, $BaMn_2As_2$ has physical properties very different from those of $BaFe_2As_2$ [11–13]. Li et al. studied the superconductivity suppression of $Ba_{0.5}K_{0.5}(Fe_{1-x}M_x)_2As_2$ single crystals by substitution of transition metal (M=Mn, Ru, Co, Ni, Cu, and Zn) [13]. Mn was observed as the strongest suppression effects, with $T_C$ suppression rate around 7.0 K/% [13]. Kim et al. used neutron and X-ray diffraction to study the antiferromagnetic ordering in $Ba(Fe_{1-x}Mn_x)_2As_2$ single crystals [12]. It was observed that for low doping concentrations, the tetragonal-to-orthorhombic transition abruptly disappears whereas magnetic ordering persists.

Although both theory and experiment indicate that the electron–phonon coupling was found to be weak to produce a superconducting state in iron-based superconductors [14, 15], the Raman light scattering offers a powerful tool to detect changes in the phonon spectra and lattice vibrations [16]. The search for specific features in the Raman spectra could shed new light onto the motive of the suppression of the

F. T. Dias
Universidade Federal de Pelotas, P. O. Box 354, Campus Universitário s/n°, 96.010-900 Pelotas, Rio Grande do Sul, Brazil

L. B. L. G. Pinheiro
Instituto Federal de Educação, Ciência e Tecnologia do Rio Grande do Sul, Campus Erechim, Rua Domingos Zanella 104, Três Vendas, 99.700-000 Erechim, Rio Grande do Sul, Brazil

A. R. Jurelo (✉)
Departamento de Física, Universidade Estadual de Ponta Grossa, Av. Gen. Carlos Cavalcanti 4748, Uvaranas, 84.030-000 Ponta Grossa, Paraná, Brazil
e-mail: arjurelo@uepg.br

superconductivity in Mn-doped $BaFe_2As_2$ single crystals [11, 12]. For $R_{1-x}K_xFe_2As_2$ (R=Ba, Sr) single crystals, it was observed from Raman scattering measurements that the electron–phonon coupling results in significant phonon anomalies at both the superconducting and spin density wave transitions [17]. Such anomalies are increasingly suppressed for higher potassium concentrations [17]. For Co-doped samples, Raman scattering measurements as a function of temperature were also used to study spin density wave (SDW) order and electron–phonon coupling in $Ba(Fe_{1-x}Co_x)_2As_2$ single crystals [18]. It was observed that the electronic Raman continuum displays clear signatures of the opening of a doping-dependent SDW gap [18]. Also, in another study involving $Ba(Fe_{1-x}Co_x)_2As_2$ single crystals, doping dependence of the lattice dynamics by Raman spectroscopy was studied [19]. A large splitting of the $E_g$ in-plane phonon modes involving Fe and As displacements was observed upon cooling through the tetragonal-to-orthorhombic transition. The origin of the splitting was discussed in terms of magnetic frustration, inherent to iron–pnictide systems [19].

In this communication, results of Raman scattering study of Mn-doped $BaFe_2As_2$ single crystals are reported. Single crystals were grown out of a FeAs self-flux using conventional high-temperature solution growth. From XRD patterns, only the (00*l*) peaks were observed, illustrating that the $Ba(Fe_{1-x}Mn_x)_2As_2$ crystals are exclusively oriented along the *c*-axis and without impurity phases detected. The AFM measurements indicated that the samples are homogeneous but shows a surface granular aspect at the nanometric scale. Raman measurements performed at room temperature and 77 K in the 45 to 1565 $cm^{-1}$ range were carried out on the *ab*- and *a*(*b*)*c*-planes. The $A_{1g}$ and $B_{1g}$ phonon modes allowed by symmetry were identified.

## 2 Experimental Details

Single crystals of $Ba(Fe_{1-x}Mn_x)_2As_2$ were grown out of a FeAs self-flux using conventional high-temperature solution growth. Details of the crystal growth process are presented elsewhere [12, 20, 21]. To determine the Mn-doping composition of the single crystals, wavelength dispersive spectroscopy was used [12]. In this work, the Mn values ($x$= 0.026, 0.052, 0.092, and 0.147) will be used to identify the single crystals. The structure and phase purity of all samples were examined using a Rigaku diffractometer with $CuK_\alpha$. The X-ray diffraction patterns were collected from 5 to 120° in the $2\theta$ range with 0.006 step and 6 s counting time. Also, the samples were characterized in different regions of the *ab*-plane by using a commercial AFM system (SPM-9600 Shimadzu) in non-contact mode. All AFM results reported in this work were obtained with silicon cantilever that has a resonant frequency of approximately 320 kHz with nominal spring constant of 42 N/m. Unpolarized confocal Raman measurements at RT and 77 K were performed with a Bruker Senterra R200-532 spectrometer equipped with an Olympus optical microscope and with a thermo-electrically cooled CCD detector. A ×50 objective microscopic lens was used to focus the laser beam (solid state laser with $\lambda$=532 nm) in different regions of the *ab*- and *a*(*b*)*c*-plane. Acquisition times ranged around 20 s with an incident laser power density below $60\times10^4$ W/$cm^2$ in order to avoid sample heating.

## 3 Results and Discussion

The shining plate-like crystals have typical dimensions ranging between 2 and 3 mm in the planar orientation and 100 μm thick. All the crystals are prone to exfoliation and easily cleaved. Figure 1 shows the X-ray diffraction pattern taken at room temperature of single crystals of $Ba(Fe_{1-x}Mn_x)_2As_2$ with (a) $x$= 0.026, (b) $x$= 0.052, (c) $x$= 0.092, and (d) $x$= 0.147. Inset of (a) shows an optical image of the single crystal. We can observe only the (00*l*) peaks, illustrating that the

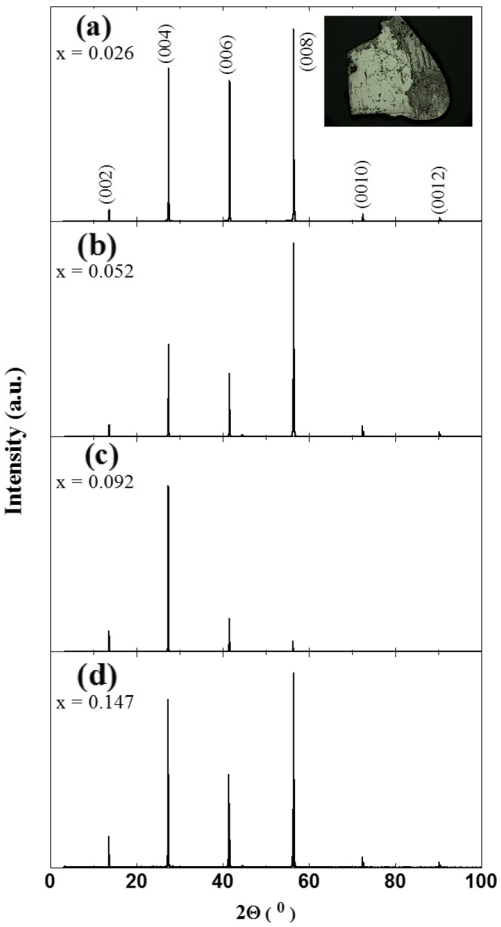


**Fig. 1** XRD patterns taken at room temperature of single crystals of $Ba(Fe_{1-x}Mn_x)_2As_2$ with **a** $x$= 0.026, **b** $x$= 0.052, **c** $x$= 0.092, and **d** $x$= 0.147. *Inset* of **a**: optical image of the doped single crystal with $x$= 0.026

$Ba(Fe_{1-x}Mn_x)_2As_2$ crystals are exclusively oriented along the *c*-axis and without impurity phases detected. However, besides the larger surface of each lamella being perpendicular to the *c*-axis, no planar ordering occurs so that each lamella can have a different orientation with respect to *a* and *b* directions. The excellent single crystals quality (for other concentrations) was also confirmed by small mosaicities [<0.02° full width at half maximum (FWHM)] measured by X-ray rocking scans [12].

In Fig. 2, Raman spectra of $Ba(Fe_{1-x}Mn_x)_2As_2$ single crystals for concentrations (a) $x=0.026$, (b) $x=0.052$, (c) $x=0.092$, and (d) $x=0.147$ are shown. The measurements were carried out in the *ab*-plane and by applying a power of 10 mW. For the sample with $x=0.026$ (Fig. 2a), a power of 20 mW was also applied and a softening for B1g mode was observed in the spectrum when compared with that obtained from 10 mW. Probably, the larger laser potency (producing locally higher temperatures) shifted the Raman peak, yet for single crystal with $x=0.147$, the measurement was also carried out at 77 K, as can be observed from Fig. 2d. The phonon modes observed in this study show typical Lorentzian lineshapes and without asymmetry.

From symmetry considerations, one expects four Raman-active phonons for $AFe_2As_2$ (where A is an alkaline earth element) [16]: $A_{1g}$ (As), $B_{1g}$ (Fe), $E_g$ (As), and $E_g$ (Fe). The alkaline earth element does not contribute to any of the Raman-active mode since it occupies a centrosymmetric position within the lattice [16]. Fe and As ions contribute for $B_{1g}$ and $A_{1g}$ modes, respectively. Displacement patterns for selected Raman-active $B_{1g}$ and $A_{1g}$ modes are shown on the left-hand side of Fig. 2. These two modes correspond to atomic displacements along the *c*-axis. *ab*-plane displacements of Fe and As are related to two $E_g$ modes, which involve motion of both atoms and are strongly mixed [16].

For $BaFe_2As_2$ single crystals, Chauvière et al. observed experimental frequencies of the Raman-active modes at room temperature in 124 $cm^{-1}$ for $E_g$ (Fe,As), 209 $cm^{-1}$ for $B_{1g}$(Fe), and 264 $cm^{-1}$ for $E_g$ (Fe,As) [19]. The $A_{1g}$ mode was not

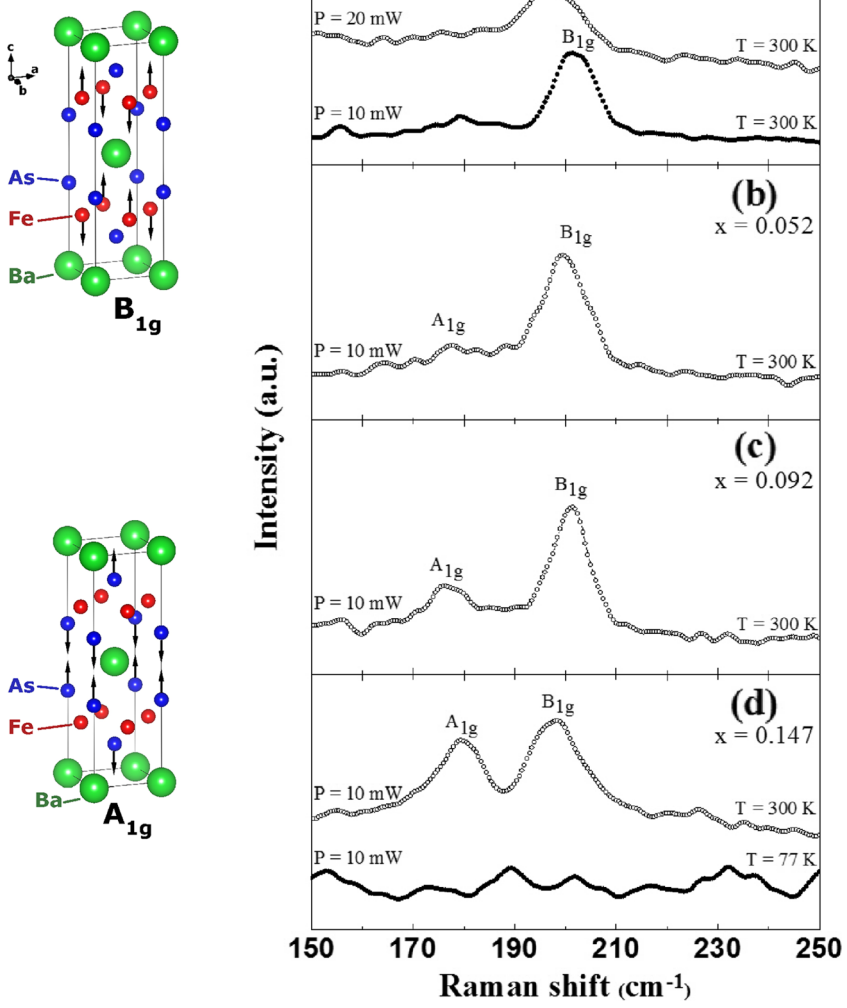


**Fig. 2** Room temperature Raman spectra of $Ba(Fe_{1-x}Mn_x)_2As_2$ for **a** $x=0.026$, **b** $x=0.052$, **c** $x=0.092$, and **d** $x=0.147$. The measurements were carried out in the *ab*-plane and by applying a power of 10 and 20 mW (only for $x=0.026$ crystal). For single crystal of $x=0.147$, the measurement was also carried out at 77 K. Displacement patterns for selected Raman-active $B_{1g}$ and $A_{1g}$ modes are also shown

observed from *ab*-plane of the $BaFe_2As_2$ single crystals. For $SrFe_2As_2$, the Raman modes were observed in 114 ($E_g$), 182($A_{1g}$), 204 ($B_{1g}$), and 264 ($E_g$) $cm^{-1}$ [16] while for the $CaFe_2As_2$ in 189 and 211 $cm^{-1}$ for $A_{1g}$ and $B_{1g}$, respectively [22].

The line observed in our study at 202 $cm^{-1}$ (correspondent to $B_{1g}$ mode) is clearly pronounced in the spectra, and its intensity and their linewidth are not dependent on Mn concentration. On the other hand, its frequency is dependent on Mn doping, as can be observed in Fig. 3. The same figure shows the room temperature Raman spectra around $B_{1g}$ line of $Ba(Fe_{1-x}Mn_x)_2As_2$ for (a) $x=0.026$ and (b) $x=0.147$. The measurements were carried out in the *ab*-plane and by applying a power of 10 mW. With increased Mn concentration, the frequency of the $B_{1g}$ phonon is reduced. The long vertical bar indicates the position of the $B_{1g}$ mode (around 202 $cm^{-1}$) for sample with $x=0.026$ while the small vertical bar indicates the position of the same mode (198 $cm^{-1}$) for the concentration $x=0.147$. The mode softens by about 4 $cm^{-1}$ with increase in Mn concentration. Chauvière et al. observed in $BaFe_2As_2$ that the $B_{1g}$ mode displays an anomaly in its linewidth at the tetragonal-to-orthorhombic transition, with a sizable decrease across the transition, while the phonon frequency of $B_{1g}$ does not exhibit any anomalies [19]. The authors argue that spin–phonon coupling can be the responsible for this anomaly [19].

The $A_{1g}$ mode could not be observed for concentration $x=0.026$ (Fig. 2a); however, this mode was clearly observed for higher concentrations of Mn. The intensity and frequency of $A_{1g}$ line depend on the concentration of Mn (Fig. 2b–d), which had its intensity and frequency increased with Mn doping. The dependence of scattering intensity and of frequency of $A_{1g}$ mode upon Mn doping might indicate that the Mn ion also occupies the As site. Chauvière et al. studied the lattice dynamics as a function of electron doping in $Ba(Fe_{1-x}Co_x)_2As_2$ by Raman spectroscopy [19]. They did not observe this mode at room temperature from measurements carried out on the *ab* in $BaFe_2As_2$ single crystals either. However, besides undetectable at RT, the $A_{1g}$ mode is clearly observed at temperatures below 147 K.

For the single crystal with $x=0.147$, the measurement was also carried out at 77 K, as can be observed from Fig. 2d. The Raman modes $A_{1g}$ and $B_{1g}$ were clearly observed at room temperature, but they could not be observed for measurements at low temperatures. Kim et al. studied the antiferromagnetic ordering in the absence of structural distortion in $Ba(Fe_{1-x}Mn_x)_2As_2$ single crystals [12]. Studies from neutron and X-ray diffraction in low doping concentrations ($x \leq 0.176$) revealed that at a critical concentration ($0.102 < x < 0.118$), the tetragonal-to-orthorhombic transition abruptly disappeared whereas magnetic ordering with a propagation vector of (1/2 ½ 1) persisted. Also, Choi et al. studied Raman scattering of $CaFe_2As_2$ at the temperature range 4–290 K [22]. For in-plane polarizations, $A_{1g}$ (at 189 $cm^{-1}$) and $B_{1g}$ (211 $cm^{-1}$) Raman-active phonon modes were observed. The $B_{1g}$ mode undergoes a discontinuous drop of frequency by 4 $cm^{-1}$, whereas the $A_{1g}$ phonon shows a suppression of the intensity at structural phase transition from the high-temperature tetragonal to the low-temperature orthorhombic phase (around $T_S \sim 173$ K). Those authors suggested that these results confirm the first-order nature of the structural phase transition and the drastic change in charge distribution within the FeAs plane through $T_S$ [22].

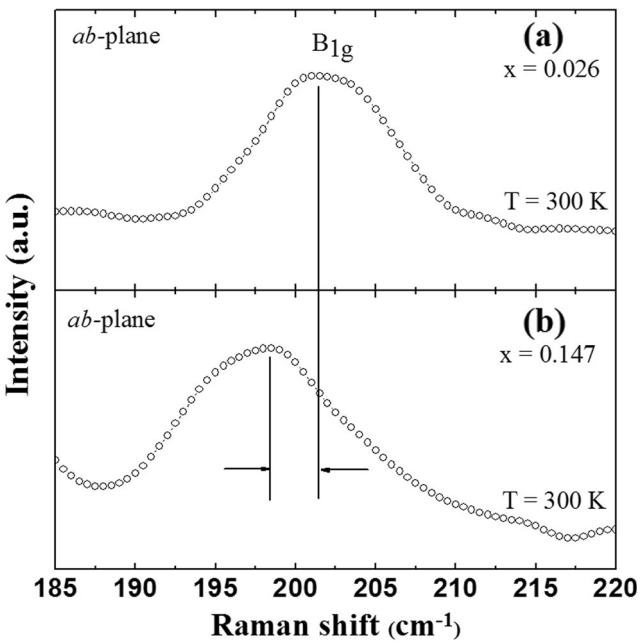


**Fig. 3** Room temperature Raman spectra around $B_{1g}$ line of $Ba(Fe_{1-x}Mn_x)_2As_2$ for **a** $x=0.026$ and **b** $x=0.147$. The measurements were carried out in the *ab*-plane and by applying a power of 10 mW

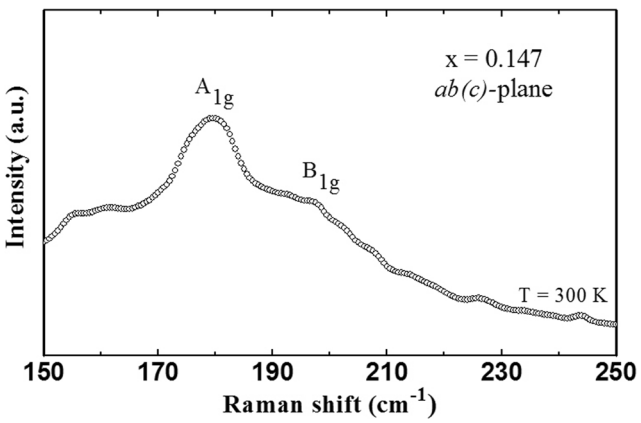


**Fig. 4** Room temperature Raman spectrum for $Ba(Fe_{1-x}Mn_x)_2As_2$($x=0.147$) for the *a(b)c*-plane at 10 mW power

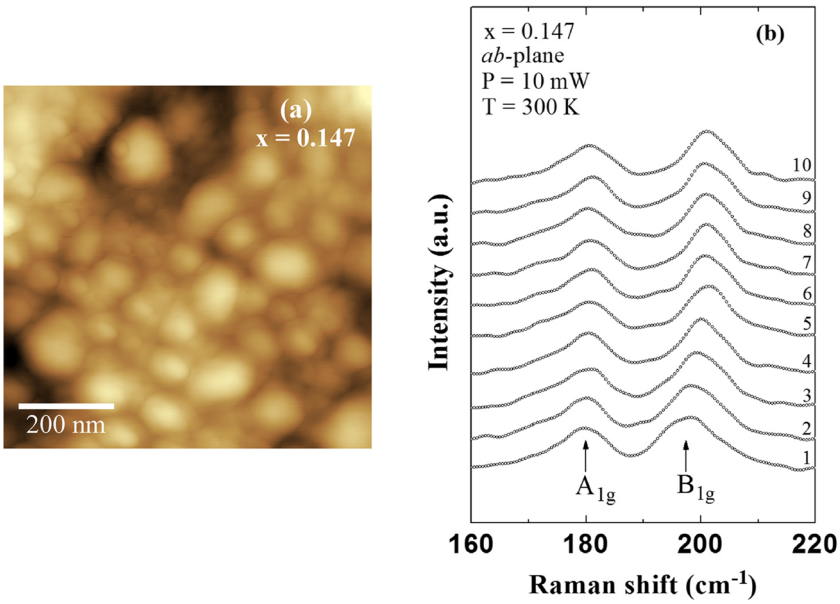


**Fig. 5** Atomic force micrograph in the *ab*-plane of $Ba(Fe_{1-x}Mn_x)_2As_2$ for **a** $x = 0.147$. **b** Lateral mapping for $x = 0.147$ in the *ab*-plane. The Raman spectra were obtained in ten steps spaced by 5 μm

Also, in this work, independent of Mn concentration and temperature, $E_g$ modes were not observed. Chauvière et al. studied the doping dependence on the lattice dynamics in $Ba(Fe_{1-x}Co_x)_2As_2$ by Raman spectroscopy [19]. They observed a large splitting of the in-plane Fe–As phonon ($E_g$) across the tetragonal–orthorhombic structural transition. They also reported that the splitting of $E_g$ mode is strongly reduced upon Co doping and disappears for $x = 0.06$. The authors discussed the origin of the splitting in terms of magnetic frustration, inherent to iron-pnictide systems, and that such enhanced splitting may be linked to strong spin–phonon coupling [19].

Figure 4 shows the room temperature Raman spectrum for $Ba(Fe_{1-x}Mn_x)_2As_2$ ($x = 0.147$) sample obtained when a 10-mW laser beam was incident on the *a(b)c*-plane. In this figure, the two Raman modes ($A_{1g}$ and $B_{1g}$) are observed again. The *a(b)c*-plane Raman modes were measured at the same frequencies as those for the *ab*-plane; therefore, $A_{1g}$ line is the most prominent, while a very weak band is observed for $B_{1g}$ mode.

Atomic force microscopy was carried out on the *ab*-plane in order to study the surface morphology of $Ba(Fe_{1-x}Mn_x)_2As_2$ sample for $x = 0.147$ (Fig. 5a). This figure shows an image of $200 \times 200$ nm$^2$ area. The image was obtained under ambient conditions in phase mode using Si probe. We did not observe changes of the examined surface by changing the AFM experimental conditions. It can be clearly observed that the sample shows a surface granular aspect, with characteristic grains sizes between 10 and 50 nm. Therefore, inhomogeneities at nanometric scale were not observed.

In order to verify the effect of granularity at nanometric scale in the Raman spectra of the $Ba(Fe_{1-x}Mn_x)_2As_2$ ($x = 0.147$) sample, several measurements were performed along ten steps of a line 50 μm long in the *ab*-plane. A laser power of 10 mW was used. The Raman spectra are shown in Fig. 5b, where the Raman modes $A_{1g}$ and $B_{1g}$ can be observed. The spectra did not change with position, showing that the sample is homogeneous despite the granularity observed from AFM measurements.

## 4 Conclusions

In conclusion, we report Raman scattering measurements on iron–pnictide non-superconducting $Ba(Fe_{1-x}Mn_x)_2As_2$ single crystals with Mn content varying from $x = 0.026$ up to 0.147. Samples were grown out of a FeAs self-flux using conventional high-temperature solution growth. From XRD, only the (00*l*) peaks were observed, illustrating that the samples are exclusively oriented along the *c*-axis and without impurity phases detected. Atomic force microscopy was carried out on the *ab*-plane in order to study the surface morphology, and it was observed that the sample shows a surface granular aspect, with characteristic grains sizes between 10 and 50 nm. Raman measurements performed at room temperature and 77 K were carried out on the *ab*- and *a*(*b*)*c*-planes. Two of four Raman-active phonons were observed experimentally. The $A_{1g}$ mode is strongly dependent upon doping of Mn, indicating possibly that the Mn ion also must be occupying the As site.

**Acknowledgments** This work was partially financed by the CNPq Brazilian Agency under contract no. 472746/2013-8. We thank to Sergey Bud'ko of the Ames Laboratory for the samples.

## References


1. Z.A. Ren, J. Yang, W. Lu, W. Yi, X.L. Shen, Z.C. Li, G.C. Che, X.L. Dong, L.L. Sun, F. Zhou, Z.X. Zhao, Europhys Lett **82**, 57002 (2008)
2. R.H. Liu, G. Wu, T. Wu, D.F. Fang, H. Chen, S.Y. Li, K. Liu, Y.L. Xie, X.F. Wang, R.L. Yang, L. Ding, C. He, D.L. Feng, X.H. Chen, Phys Rev Lett **101**, 87001 (2008)
3. M. Rotter, M. Pangerl, M. Tegel, D. Johrendt, Angew Chem Int Ed **47**, 7949 (2008)
4. F.C. Hsu, J.Y. Luo, K.W. Yeh, T.K. Chen, T.W. Huang, P.M. Wu, Y.C. Lee, Y.L. Huang, Y.Y. Chu, D.C. Yan, M.K. Wu, Proc Natl Acad Sci **105**, 14262 (2008)
5. J.H. Tapp, Z. Tang, B. Lv, K. Sasmal, B. Lorenz, P.C.W. Chu, A.M. Guloy, Phys Rev B **78**, 60505 (R) (2008)
6. X.C. Wang, Q.Q. Liu, Y.X. Lv, W.B. Gao, L.X. Yang, R.C. Yu, F.Y. Li, C.Q. Jin, Solid State Commun **148**, 538 (2008)
7. M.J. Pitcher, D.R. Parker, P. Adamson, S.J.C. Herkelrath, A.T. Boothroyd, R.M. Ibberson, M. Brunelli, S.J. Clarke, Chem Commun **2008**, 5918 (2008)
8. M. Rotter, M. Tegel, D. Johrendt, Phys Rev Lett **101**, 107006 (2008)
9. K. Sasmal, B. Lv, B. Lorenz, A. M. Guloy, F. Chen, Y. Y. Xue, C. W. Chu, arXiv: 0806.1301
10. A.S. Sefat, R. Jin, M.A. McGuire, B.C. Sales, D.J. Singh, D. Mandrus, Phys Rev Lett **101**, 117004 (2008)
11. D.C. Johnston, Advances in Physics **59**(6), 803 (2010)
12. M.G. Kim, A. Kreyssig, A. Thaler, D.K. Pratt, W. Tian, J.L. Zarestky, M.A. Green, S.L. Bud'ko, P.C. Canfield, R.J. McQueeney, A.I. Goldman, Phys Rev B **82**, 220503(R) (2010)
13. J. Li, Y. F. Guo, S. B. Zhang, J. Yuan, Y. Tsujimoto, X. Wang, C. I. Sathish, Y. Sun, S. Yu, W. Li, K. Yamaura, E. Takayama-Muromachiu, Y. Shirako, M. Akaogi, H. Kontain, arXiv: 1206.0811
14. L. Boeri, O.V. Dolgov, A.A. Golubov, Phys Rev Lett **101**, 26403 (2008)
15. R.H. Liu, T. Wu, G. Wu, H. Chen, X.F. Wang, Y.L. Xie, J.J. Ying, Y.J. Yan, Q.J. Li, B.C. Shi, W.S. Chu, Z.Y. Wu, X.H. Chen, Nature **459**, 64 (2009)
16. A.P. Litvinchuk, B. Lv, C.W. Chu, Phys Rev B **84**, 092504 (2011)
17. M. Rahlenbeck, G.L. Sun, D.L. Sun, C.T. Lin, B. Keimer, C. Ulrich, Phys Rev B **80**, 64509 (2009)
18. L. Chauvière, Y. Gallais, M. Cazayous, M.A. Méasson, A. Sacuto, D. Colson, A. Forget, Phys Rev B **84**, 104508 (2011)
19. L. Chauvière, Y. Gallais, M. Cazayous, A. Sacuto, M.A. Méasson, D. Colson, A. Forget, Phys Rev B **80**, 94504 (2009)
20. N. Ni, M.E. Tillman, J.Q. Yan, A. Kracher, S.T. Hannahs, S.L. Bud'ko, P.C. Canfield, Phys Rev B **78**, 214515 (2008)
21. P.C. Canfield, S.L. Bud'ko, Annu Rev Condens Matter Phys **1**, 27 (2010)
22. K.Y. Choi, D. Wulferding, P. Lemmens, N. Ni, S.L. Budko, P.C. Canfield, Phys Rev B **78**, 212503 (2008)